

1 *Supplementary of*

2 **Numerical modeling on the mechanisms of chlorine chemistry in snowpack and**
3 **their impact on secondary atmospheric pollution**

4

5

6 **Shengjin Xie et al.**

7

8 Correspondence to: Xuelei Zhang (zhangxuelei@iga.ac.cn)

9

10

11 **This supplementary document consists of including 2 text, 6 Figures and 3 Tables.**

12

Text captions

13 **Text S1.** N₂O₅ uptake and ClNO₂ production on snowpack.

14 **Text S2.** Snow parameters observed by satellite remote sensing.

15

16

Figure captions

17 **Figure S1.** Characterization of S/V_g under different LU-LC.

18 **Figure S2.** N₂O₅ uptake and ClNO₂ yield on the ground surfaces (snow, vegetation,
19 and buildings).

20 **Figure S3.** Monthly average spatial distribution of snow parameters (snow depth, snow
21 coverage, snow density, and albedo).

22 **Figure S4.** Spatial distribution of oxidative species (OH, HO₂, RO₂) in different
23 scenarios.

24 **Figure S5.** Spatial distribution of PM_{2.5} and its component species in different scenarios.

25 **Figure S6.** The contribution of the photolysis process of ClNO₂ on the ground surface.

26

27

Table captions

28 **Table S1.** Model configurations of WRF and CAMx.

29 **Table S2.** Heterogeneous chemical reaction parameter schemes of N₂O₅ on aerosol
30 surface.

31 **Table S3.** Comparative analysis of statistical indicators for the simulation results of

32 N₂O₅ heterogeneous processes on atmospheric aerosol surfaces under different
33 parameter schemes.

34

35

Text captions

36 **Text S1. N₂O₅ uptake and ClNO₂ Production on snowpack:**

37 Previous studies in mid-latitude regions report a snow particle radius (r_s) near the
38 surface ranging from 40 to 500 μm , with snow density between 0.14 and 0.26 g cm^{-3}
39 (Wang et al., 2020). The Northeast China region exhibits a larger snow particle size
40 range (370-1550 μm) and lower snow density (0.07-0.21 g cm^{-3}). Compared with the
41 above data, we sampled a snow particle radius of 600 μm within the existing research
42 range and used a snow density of 0.20 g cm^{-3} for study. The calculated snow specific
43 surface area is 54 $\text{cm}^2 \text{g}^{-1}$.

44 The pseudo first order loss rate of N₂O₅ (g) on snow grain is shown in equation
45 (R1-R2).

$$46 \quad \frac{d[\text{N}_2\text{O}_5]}{dt} = -k_{het}[\text{N}_2\text{O}_5] \quad (\text{R1})$$

$$47 \quad k_{het} = \frac{1}{4} \gamma_{eff, \text{N}_2\text{O}_5} \bar{v} \times SA \quad (\text{R2})$$

$$48 \quad \frac{1}{\gamma_{eff, \text{N}_2\text{O}_5}} = \frac{1}{\Gamma_{diff}} + \frac{1}{\gamma_{\text{N}_2\text{O}_5, snow}} \quad (\text{R3})$$

$$49 \quad \frac{1}{\Gamma_{diff}} = \frac{8D_{SIA}}{\bar{v}(2r)} \quad (\text{R4})$$

50 k_{het} is the pseudo-first-order rate coefficient, $\gamma_{eff, \text{N}_2\text{O}_5}$ is the effective uptake
51 coefficient, \bar{v} (cm s^{-1}) is the thermal speed, and SA is the ratio of ground surface (snow
52 grain) to volume. $\gamma_{\text{N}_2\text{O}_5, snow}$ and $\gamma_{eff, \text{N}_2\text{O}_5}$ are the reactive uptake and the effective
53 uptake coefficient of N₂O₅ on snow grains, respectively. Γ_{diff} is a correction term for
54 normalized gas-diffusion rate. r is the snow grain radius.

55 The diffusion rate in snow interstitial air (SIA) is controlled by molecular diffusion
56 D_{SIA} ($\text{m}^2 \text{s}^{-1}$) (Thomas et al., 2011; Toyota et al., 2014; Wang et al., 2020). D_g is the
57 diffusion coefficient. λ_{air} is the mean free path. τ is the snow tortuosity ($\tau = 2$) (Wang
58 et al., 2020).

59
$$D_{SIA} = \frac{D_g}{\tau} \quad (R5)$$

60
$$D_g = \frac{1}{3} \lambda_{air} \sqrt{8RT/(M\pi)} \quad (R6)$$

61 The liquid brine layer fraction (f_{brine}) in a sodium chloride solution is estimated by Eq.
 62 R7 , reflecting the enrichment of Na and Cl^- in the snow-brine layer (Cho et al., 2002).
 63 The f_{brine} , a highly concentrated salt solution, typically resides within the pores between
 64 ice crystals and should not be equated with the direct measurement of chloride ion
 65 concentration in snow meltwater samples. $[Cl^-](M)$ represents the chloride
 66 concentration in the snow brine phase, which is estimated by dividing the snow melt
 67 chloride concentrations by f_{brine} . M_{H_2O} is the molecular weight of water, R is the gas
 68 constant, T_f is the freezing temperature, ΔH_f^0 is the enthalpy of fusion, and C_T is the
 69 total concentration of ions of the snowmelt sampled on the corresponding day.

70
$$f_{brine} = \frac{M_{H_2O} R T_f}{1000 \Delta H_f^0} \left(\frac{T}{T - T_f} \right) C_T \quad (R7)$$

71
$$\frac{1}{\gamma} = \frac{1}{\alpha} + \frac{\bar{v}}{4HRT \sqrt{k^l D_{aq}}} \quad (R8)$$

72 k^l is the pseudo-first-order rate in the brine layer. and D_{aq} is the aqueous diffusion
 73 coefficient. The $ClNO_2$ yield from snow grains ($Y_{ClNO_2, snow}$) were calculated. The
 74 parameters in k^l and $Y_{ClNO_2, snow}$ can be found in (Wang et al., 2020).

75
$$k^l = k_{H_2O} [H_2O] + k_{Cl^-} [Cl^-] \quad (R9)$$

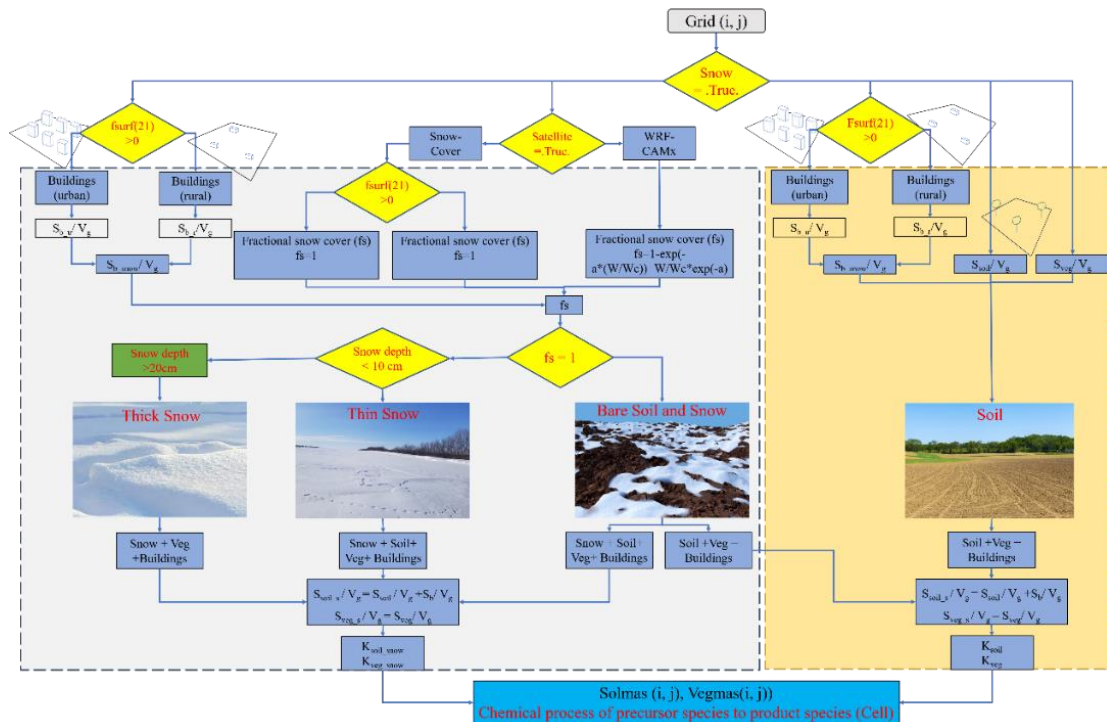
76
$$Y_{ClNO_2, snow} = \frac{k_{Cl^-} [Cl^-]}{k_{Cl^-} [Cl^-] + k_{H_2O} [H_2O]} \quad (R10)$$

77 **Text S2. Snow parameters observed by satellite remote sensing.**

78 The snow parameters (depth, snow-cover, density, and albedo) were extracted
 79 from the ERA5.0 dataset to calculate monthly average spatial distribution maps for
 80 February 2024 (Fig. S3). In Northeast China, the maximum monthly average snow
 81 depth reached 0.7 m in southeastern Heilongjiang Province. Snow depth generally
 82 increased with increasing latitude across the region. Snow coverage exceeded 95% in
 83 most areas of Heilongjiang Province and parts of southeastern Jilin Province.
 84 Conversely, snow coverage was relatively low (15-30%) in western Jilin Province and

85 the central and southwestern regions of Liaoning Province. In areas with high snow
 86 depth and coverage in Heilongjiang Province, maximum snow density reached 254
 87 kg/m³. In other regions, snow density remained relatively constant at approximately
 88 135 kg/m³ (Fig. S3c), consistent with the snow density range reported in the (Text S1).
 89 The reliability of the observed 0.2 g cm⁻³ (200 kg/m³) snow density was further
 90 validated using satellite data. Maximum snow albedo values reached approximately
 91 0.73, exhibiting a correlation with snow depth snow age. This analysis presents the
 92 spatial distribution of snow parameters based on monthly averages (Figure S3b).
 93 However, it is crucial to acknowledge potential biases arising from snowmelt events,
 94 which could result in soil exposure and inaccuracies in the assessment of true snow
 95 cover conditions. The numerical range of snow variables provided by the ERA5.0
 96 reanalysis data was utilized to verify the accuracy of snow depth, coverage, and density
 97 data obtained through field observations and laboratory physical tests in the Text S1.
 98 This validation step ensured the accuracy and effectiveness of the simulation results
 99 under regional snow conditions.

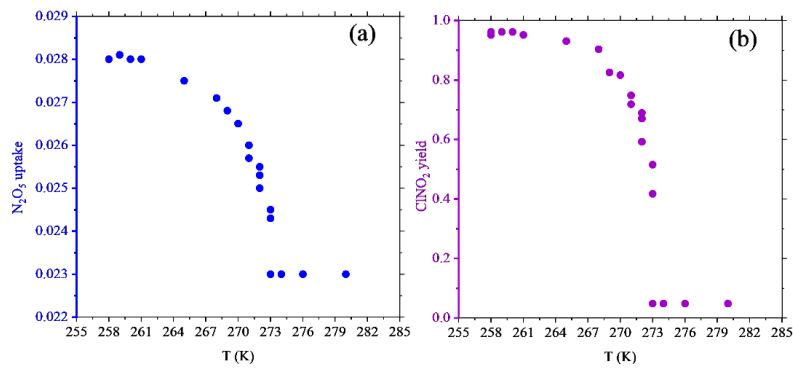
100 **Figure captions**



101

102

Figure S1. Characterization of S/V_g under different LU-LC.



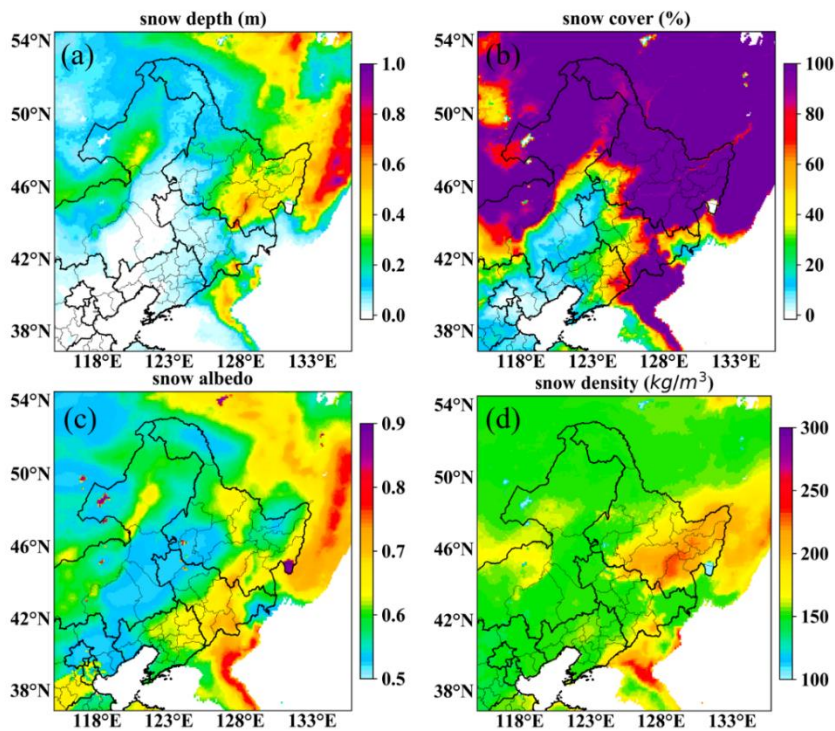
103

104

Figure S2. N_2O_5 uptake and $ClNO_2$ yield on the ground surfaces (snow, vegetation, and buildings).

105

106

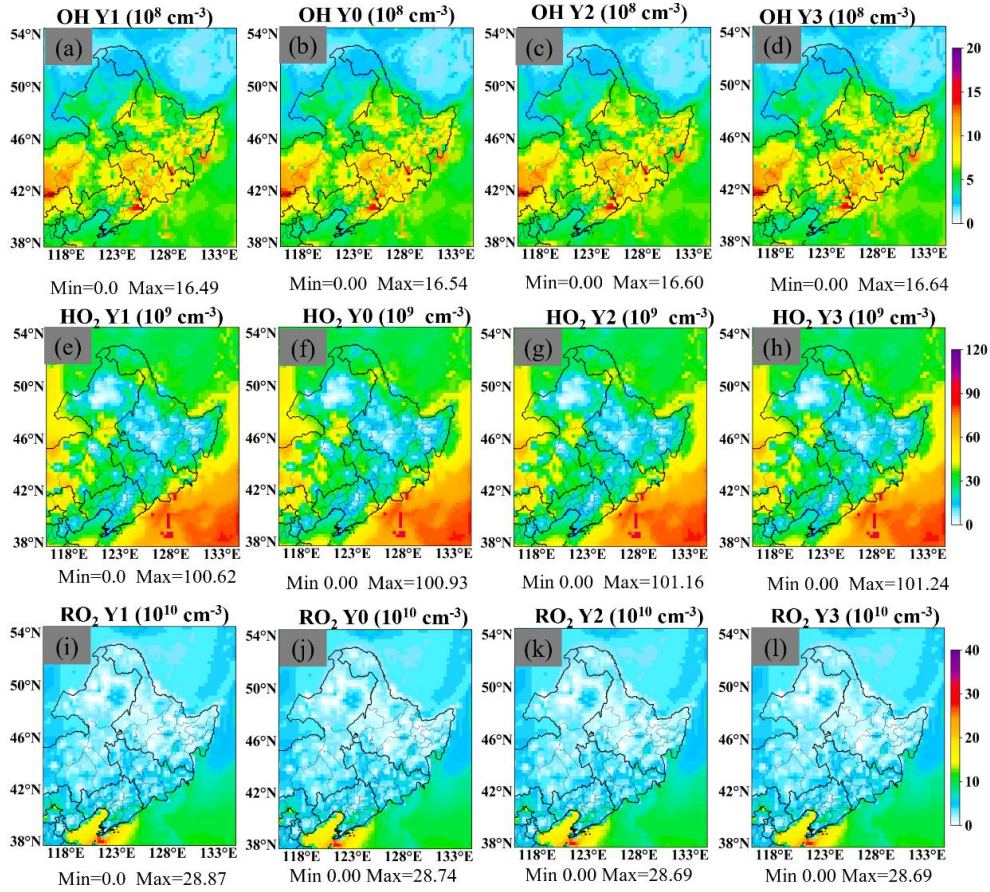


107

108

Figure S3. Monthly average spatial distribution of snow parameters (snow depth, snow coverage, snow density, and albedo).

109

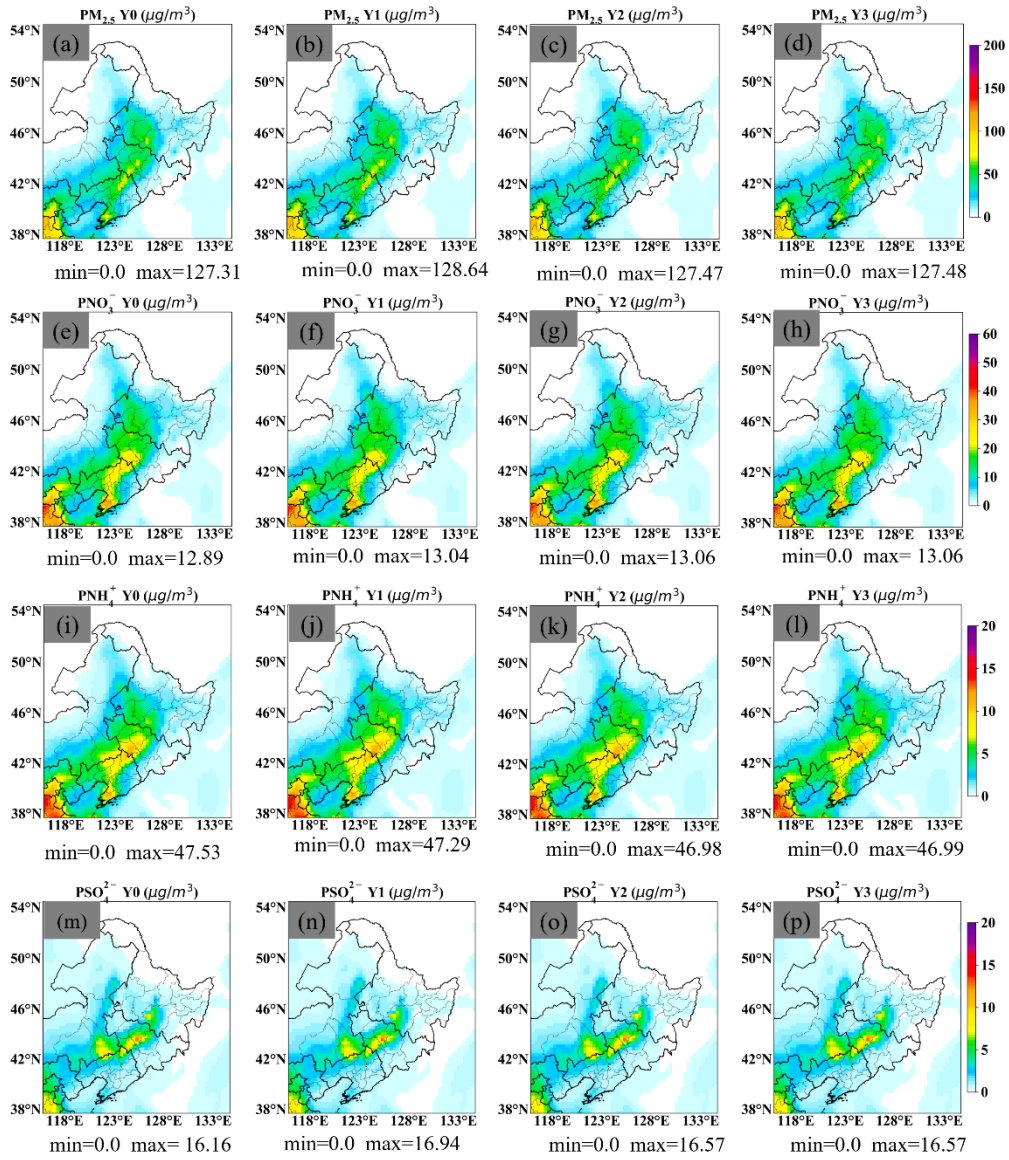


110

111

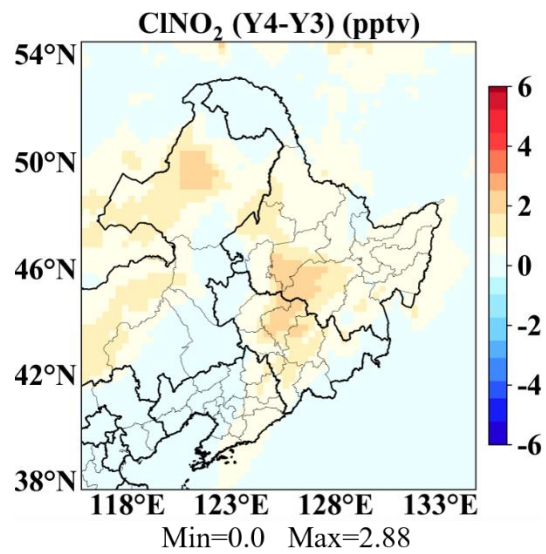
Figure S4. Spatial distribution of oxidative species (OH, HO₂, and RO₂) in different scenarios.

112



113

114 **Figures S5.** Spatial distribution of $PM_{2.5}$ and its component species in different
 115 scenarios.



116

117 **Figure S6.** The contribution of the photolysis process of CINO₂ on the ground surface

118

Table captions

119

Table S1. Model configurations of WRF and CAMx

WRFv3.9.1 Model Configurations		CAMxv7.10 Model Configurations	
Physics Treatment	Scheme	Model options	Scheme
Microphysics	(6) WSM6	Vertical diffusion	ACM2
Longwave radiation	(4) RRTMG	Horizontal diffusion	Explicit simultaneous 2-D solver
Shortwave radiation	(4) RRTMG	Vertical advection	PPM
Land surface model (LSM)	(2) Noah Land-Surface	Horizontal Advection	PPM
Surface layer	(1) Monin-Obukhov	Chemistry Solver	EBI
Planetary boundary layer scheme	(1) YSU	Deposition velocity	ZHANG03
Cumulus Parameterization	(5) Grell 3D	Gas-phase chemistry / Aerosol module	CB06/ CF

120

Table S2. Heterogeneous chemical reaction parameter scheme of N₂O₅ on aerosol surface

122

Parameter	CAMx	Yu (2020)
	Bertram (2009)	
Source	Laboratory simulation	Field observations (China)
k'_{2f}	$\beta - \beta e^{-\delta[H_2O]}$	$3.0 \times 10^4 \times [H_2O]$
k_3/k_{2b}	0.06	0.033
k_4/k_{2b}	29	3.4
k_4/k_3	483	103

123

Table S3. Comparative analysis of statistical indicators for the simulation results of N₂O₅ heterogeneous processes on atmospheric aerosol surfaces under different parameter schemes

126

Pollutants	Snow	Schemes	MB (pptv)	NMB (%)	RMSE (pptv)	IOA
N ₂ O ₅	✓	BT09	114.64	1.92	201.39	0.49
	✓	YU20	69.66	1.16	139.03	0.61
ClNO ₂	✓	BT09	-29.28	-0.28	100.66	0.81
	✓	YU20	-16.08	-0.16	99.80	0.84

127

128

References

130

131 Cho, H., Shepson, P. B., Barrie, L. A., Cowin, J. P., and Zaveri, R.: NMR investigation of the quasi-brine
 132 layer in ice/brine mixtures, *The Journal of Physical Chemistry B*, 106, 11226-11232,
 133 <https://doi.org/10.1021/jp020449+>, 2002.

134 Thomas, J. L., Stutz, J., Lefer, B., Huey, L. G., Toyota, K., Dibb, J. E., and von Glasow, R.: Modeling
 135 chemistry in and above snow at Summit, Greenland - Part 1: Model description and results, *Atmos.*

136 Chem. Phys., 11, 4899-4914, <https://doi.org/10.5194/acp-11-4899-2011>, 2011.

137 Toyota, K., McConnell, J. C., Staebler, R. M., and Dastoor, A. P.: Air – snowpack exchange of bromine,
138 ozone and mercury in the springtime Arctic simulated by the 1-D model PHANTAS – Part 1: In-snow
139 bromine activation and its impact on ozone, Atmos. Chem. Phys., 14, 4101-4133,
140 <https://doi.org/10.5194/acp-14-4101-2014>, 2014.

141 Wang, S., McNamara, S. M., Kolesar, K. R., May, N. W., Fuentes, J. D., Cook, R. D., Gunsch, M. J.,
142 Mattson, C. N., Hornbrook, R. S., Apel, E. C., and Pratt, K. A.: Urban Snowpack ClNO₂ Production
143 and Fate: A One-Dimensional Modeling Study, ACS Earth Space Chem., 4, 1140-1148,
144 10.1021/acsearthspacechem.0c00116, <https://doi.org/10.1021/acsearthspacechem.0c00116>, 2020.